



Spin-flip configuration interaction singles with exact spin-projection: Theory and applications to strongly correlated systems

Tsuchimochi, Takashi

(Citation)

Journal of Chemical Physics, 143(14):144114-144114

(Issue Date)

2015-10-14

(Resource Type)

journal article

(Version)

Version of Record

(Rights)

©2015 American Institute of Physics. This article may be downloaded for personal use only. Any other use requires prior permission of the author and the American Institute of Physics. The following article appeared in Journal of Chemical Physics 143(14), 144114 and may be found at <http://dx.doi.org/10.1063/1.4933113>

(URL)

<https://hdl.handle.net/20.500.14094/90002924>



Spin-flip configuration interaction singles with exact spin-projection: Theory and applications to strongly correlated systems

Takashi Tsuchimochi

Citation: *The Journal of Chemical Physics* **143**, 144114 (2015); doi: 10.1063/1.4933113

View online: <http://dx.doi.org/10.1063/1.4933113>

View Table of Contents: <http://scitation.aip.org/content/aip/journal/jcp/143/14?ver=pdfcov>

Published by the [AIP Publishing](#)

Articles you may be interested in

[Configuration interaction singles natural orbitals: An orbital basis for an efficient and size intensive multireference description of electronic excited states](#)

J. Chem. Phys. **142**, 024102 (2015); 10.1063/1.4905124

[Restricted active space spin-flip configuration interaction: Theory and examples for multiple spin flips with odd numbers of electrons](#)

J. Chem. Phys. **137**, 164110 (2012); 10.1063/1.4759076

[Avoided crossings, conical intersections, and low-lying excited states with a single reference method: The restricted active space spin-flip configuration interaction approach](#)

J. Chem. Phys. **137**, 084105 (2012); 10.1063/1.4747341

[Strongly correlated mechanisms of a photoexcited radical reaction from the anti-Hermitian contracted Schrödinger equation](#)

J. Chem. Phys. **134**, 034111 (2011); 10.1063/1.3526298

[Determination of spin Hamiltonians from projected single reference configuration interaction calculations. I. Spin 1/2 systems](#)

J. Chem. Phys. **133**, 044106 (2010); 10.1063/1.3458642



AIP | APL Photonics

APL Photonics is pleased to announce
Benjamin Eggleton as its Editor-in-Chief



Spin-flip configuration interaction singles with exact spin-projection: Theory and applications to strongly correlated systems

Takashi Tsuchimochi^{a)}
 Department of Computational Science, Graduate School of System Informatics, Kobe University,
 Kobe 657-8501, Japan

(Received 24 July 2015; accepted 1 October 2015; published online 14 October 2015)

Spin-flip approaches capture static correlation with the same computational scaling as the ordinary single reference methods. Here, we extend spin-flip configuration interaction singles (SFCIS) by projecting out intrinsic spin-contamination to make it spin-complete, rather than by explicitly complementing it with spin-coupled configurations. We give a general formalism of spin-projection for SFCIS, applicable to any spin states. The proposed method is viewed as a natural unification of SFCIS and spin-projected CIS to achieve a better qualitative accuracy at a low computational cost. While our wave function *ansatz* is more compact than previously proposed spin-complete SF approaches, it successfully offers more general static correlation beyond biradicals without sacrificing good quantum numbers. It is also shown that our method is invariant with respect to open-shell orbital rotations, due to the uniqueness of spin-projection. We will report benchmark calculations to demonstrate its qualitative performance on strongly correlated systems, including conical intersections that appear both in ground-excited and excited-excited degeneracies. © 2015 AIP Publishing LLC. [<http://dx.doi.org/10.1063/1.4933113>]

I. INTRODUCTION

In electronic structure theory, static correlation is the essential part of electron correlation, without which even a qualitative description of a system cannot be made possible. The major break-down of conventional single reference methods is often traced to its inability to treat static correlation in many chemically important molecular systems, especially those with distorted geometries such as bond dissociation processes. This failure is due to the fact that the nature of the wave functions of such systems is multireference, i.e., multiple determinants gain comparable weights. Unfortunately, most single reference methods that stem from Hartree-Fock (HF) fail to describe this important feature,¹ and the search for cost-effective multireference methods is currently an active research area in quantum chemistry.^{2–7}

Among several multireference methods, a variety of spin-flip (SF) approaches have become popular in the last decade because of their simplicity and favorable computational scalings (same as the conventional non-SF methods).^{8–16} They are based on a single concept that the electron excitations considered in each method are spin-flipped from a high-spin $m + 1$ state, i.e., $\alpha \rightarrow \beta$, to give a multireference $|s; m\rangle$ state, where s and m indicate the quantum numbers associated with \hat{S}^2 and \hat{S}_z , respectively. A high-spin reference is more suitable to start with, since there is no entanglement between degenerate open-shell orbitals in principle. This scheme was later extended to density functional theory.^{17–20}

Even the simplest SF model based on configuration interaction singles (CIS), termed SFCIS, successfully accounts for a biradical character such as single bond dissociation

and ethylene torsion.^{8,9} Hence, SF approaches have attracted widespread interest in the community and have been applied to many chemically relevant systems that exhibit unusual static correlation.^{21–25} However, there are two main issues with SF methods. First, the resultant states are not a spin eigenfunction in general.¹¹ It is usually observed that the excited states, and in many cases the ground state, are significantly spin-contaminated, that is, they are a mixture of $s = m, m + 1$, and even higher spin states. As notoriously known, large spin-contamination can easily cause not only inaccurate excitation energies but also lead to incorrect assignment of spectrum.^{26–28} Note that use of a restricted open-shell HF (ROHF) reference still suffers from the same issue, because it is attributed to the neglect of spin-coupled counterparts of the SF-configuration space. There have been attempts to overcome this deficiency by expanding the CI space to complete the spin-adapted configuration state functions (CSFs).^{11,15} It was shown that such spin-complete SFCIS (SC-SFCIS) improved the results over SFCIS in many aspects. However, as we shall see, SC-SFCIS turned out to be not invariant with respect to orbital rotations and the ground state energy is thus affected by the choice of open-shell orbitals rather significantly. The second problem in the current SF models, which is also widely known in the community, is their inability of treating systems where a more general description of static correlation is required. In other words, SFCIS is unable to dissociate a multiple bond correctly, since it only takes into account some of the doubly excited configurations at most and misses higher order excitations. Along this line, Casanova *et al.* have proposed to use an $m + 2$ reference and perform double SF excitations.²⁹ This approach was shown to be more powerful than single SF methods but is still limited to double bond dissociation. A more general strategy for multiradicals is to allow an arbitrary

^{a)}tsuchimochi@gmail.com

number of SF excitations in conjunction with restricted active spaces.^{30–33} Alternatively, one could use a symmetry-broken reference state at the cost of introducing further spin-contamination; however, this would drastically deteriorate the computed excitation energies, and the advantage of SF models would be thus completely lost.

In this article, we will address these issues from a different view point, by applying the spin-projection operator.^{34–38} Through the spin-projection operator, one can obtain faithful descriptions of spin-adapted SF states. As we will see, this procedure offers invariance of a wave function with respect to orbital rotations. Furthermore, one can employ a heavily spin-contaminated reference state to account for residual static correlation beyond the HOMO-LUMO degeneracy. The proposed method is also realized as a natural extension of spin-projected CIS (PCIS), where spin-projected configurations are used as the CI basis,^{28,39} and therefore hereafter will be called SFPCIS. Although PCIS was shown to be promising for degenerate molecular systems, it is not without its own problems. That is, it cannot account for some low-lying excitations which often require double-substitutions in strongly correlated systems. Moreover, due to the generalized Brillouin theorem, single-substituted projected determinants cannot mix with the reference ground state.^{28,40} This is indeed a serious drawback of PCIS because a conical intersection and avoided crossing between the *ground* state and an excited state cannot be described properly, as is the case in regular CIS as well as time-dependent density functional theory.⁴¹ While these problems are mainly attributed to the absence of doubles (and triples, so on) in the PCIS model and could be eventually solved by incorporating higher excitations, we will show that SFPCIS can be a good compromise, providing a better approximation to degenerate systems at a cost comparable to SFCIS.

This paper is organized as follows. In Section II, we will briefly review SFCIS and SC-SFCIS approaches and then introduce spin-projection. Orbital invariance property and size-intensivity of SFPCIS are also discussed in detail. Section IV reports some benchmark calculations of SFPCIS on small molecules and compares the *qualitative* performance of each method. Finally, our conclusions are drawn in Section V.

II. THEORY

A. Spin-flip CIS and its extension

Let $|\Phi\rangle$ be a reference high-spin state with $S_z = m + 1$ with m being the target spin state. In SFCIS, one variationally optimizes the following wave function *ansatz*:

$$|\Psi^{\text{SFCIS}}\rangle = \sum_{ai} c_{ai} |\Phi_i^{\bar{a}}\rangle. \quad (1)$$

We will use the conventional orbital notations: i, j, \dots for occupied orbitals, a, b, \dots for virtual orbitals, and p, q, \dots for general orbitals. A bar indicates a beta spin orbital. Hence, in SFCIS, one considers SF transitions from an α occupied orbital to a β virtual orbital.⁸ In Figure 1, we summarize the main configurations generated by SF excitations from a high-spin triplet determinant, either ROHF or unrestricted HF (UHF) reference (thus, spatial orbitals can be different for

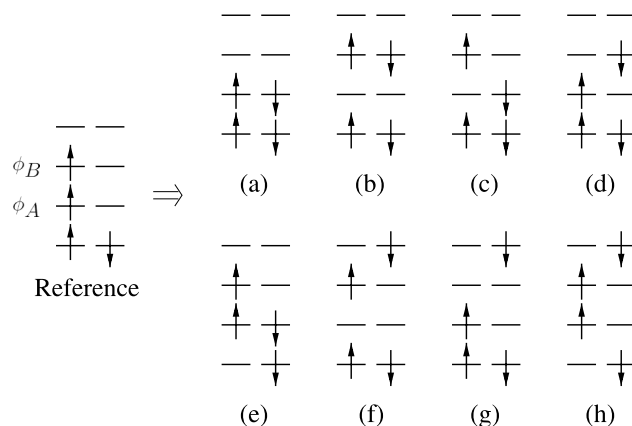


FIG. 1. Spin-flip single excitations from a triplet reference determinant.

α and β spins). Configurations (a) and (b) are the ones that become essential for static correlation when ϕ_A and ϕ_B are nearly degenerate, and SFCIS takes them into account in a balanced manner.

It should be clear that, in general, $\hat{S}_z |\Psi^{\text{SFCIS}}\rangle = m |\Psi^{\text{SFCIS}}\rangle$ but $\hat{S}^2 |\Psi^{\text{SFCIS}}\rangle \neq s(s+1) |\Psi^{\text{SFCIS}}\rangle$ even with a ROHF reference, because configurations (e)–(h) are largely spin-contaminated (while (c) and (d) can be coupled together to form a singlet). These determinants need spin-coupled counterparts to complete the correct spin. Namely, (g) is a mixture of a singlet $|\Psi_0^S\rangle$ and a triplet $|\Psi_0^T\rangle$ and constitutes the former together with (g1) (shown in Fig. 2). Determinant (h) is further contaminated with a quintet state and is associated with *two* singlet states, $|\Psi_1^S\rangle$ and $|\Psi_2^S\rangle$.⁴² Based on this observation, Sears and coworkers attempted to complete spin-states in SFCIS by adding extra determinants, namely, (g1) and (h1)–(h5), and investigated the consequence of using such a spin-complete basis.¹¹ This so-called SC-SFCIS was shown to yield encouraging results

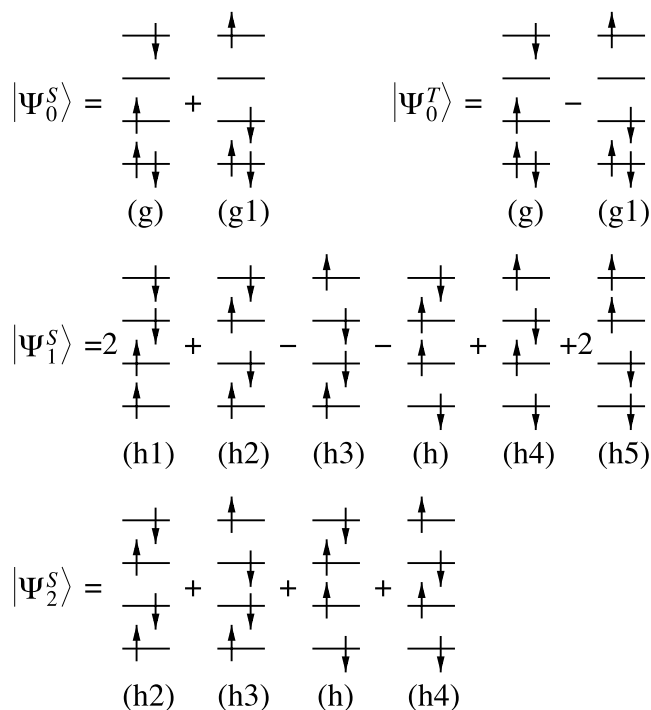


FIG. 2. CSFs generated by spin-coupled counterparts.

TABLE I. Property and capability of each method.

	SFCIS	SC-SFCIS	SF-XCIS	PCIS	SFPCIS/ROHF	SFPCIS/PHF
Spin-complete		✓	✓	✓	✓	✓
Orbital invariant	✓		✓	✓	✓	✓
Size-intensive	✓	✓	✓		✓	
Doublet states	✓			✓	✓	✓
Conical intersection	✓	✓	✓		✓	✓
Multiradical character ^a				✓		✓

^aIn a broader sense than just bi- and triradicals.

for both the ground and excited states compared to SFCIS. However, currently SC-SFCIS is limited to a triplet reference, and for other reference, e.g., quartet, one has to reformulate the method to deal with somewhat more complicated CSFs.

In what follows, we will let spin-projection do this configuration selection. The spin-projection operator automatically generates the associated CSF from a spin-incomplete determinant.

B. Spin-projection model

We first introduce the spin projection operator $\hat{P}^s \equiv |s; m\rangle\langle s; m|$ to eliminate undesired spin-contamination,^{35–38}

$$\hat{P}_{mm}^s = \frac{2s+1}{8\pi^2} \int_{\Omega} d\Omega e^{i\alpha m} d_{mm}^{s*}(\beta) e^{i\gamma m} \hat{R}(\Omega), \quad (2)$$

$$\hat{R}(\Omega) = e^{-i\alpha \hat{S}_z} e^{-i\beta \hat{S}_y} e^{-i\gamma \hat{S}_z}, \quad (3)$$

where Ω stands for a set of Euler angles (α, β, γ) , and $d_{mm}^s(\beta)$ is the so-called Wigner small d-matrix. Note that this form is computationally much more tractable than Löwin's spin-projection operator,³⁴ which has been extensively used in quantum chemistry for decades.^{43–47}

Applying Eq. (2) to a broken-symmetry UHF wave function, and minimizing its energy variationally, we obtain the so-called variation-after-projection (VAP) solution. Such an approach is also referred to as spin-projected UHF (SUHF) in the recent literature, which is a subset of projected HF (PHF) — a more general framework that uses several projection operators.³⁸ Since in this work we are only concerned with spin-projection, we use PHF to specifically mean SUHF throughout this paper. We will also omit subscripts m in Eq. (2) for brevity.

Now we are in position to define the SFPCIS *ansatz*,

$$|\Psi^{\text{SFPCIS}}\rangle = \hat{P}^s \sum_{\bar{a}\bar{i}} c_{\bar{a}\bar{i}} |\Phi_{\bar{i}}^{\bar{a}}\rangle. \quad (4)$$

SFPCIS is exactly the same as SFCIS, except that all the determinants in Figure 1 are now explicitly spin-projected. Also, it should be pointed out that $c_{\bar{a}\bar{i}}$ are variationally determined by solving the following non-orthogonal CI equation:

$$\mathbf{H}\mathbf{c} = E\mathbf{N}\mathbf{c}, \quad (5)$$

where the matrix elements are defined as

$$H_{j\bar{b}}^{i\bar{a}} = \langle \Phi_{\bar{i}}^{\bar{a}} | \hat{P}^{s\dagger} \hat{H} \hat{P}^s | \Phi_{\bar{j}}^{\bar{b}} \rangle = \langle \Phi_{\bar{i}}^{\bar{a}} | \hat{H} \hat{P}^s | \Phi_{\bar{j}}^{\bar{b}} \rangle, \quad (6)$$

$$N_{j\bar{b}}^{i\bar{a}} = \langle \Phi_{\bar{i}}^{\bar{a}} | \hat{P}^{s\dagger} \hat{P}^s | \Phi_{\bar{j}}^{\bar{b}} \rangle = \langle \Phi_{\bar{i}}^{\bar{a}} | \hat{P}^s | \Phi_{\bar{j}}^{\bar{b}} \rangle. \quad (7)$$

Here, we have used the fact that \hat{P}^s is Hermitian, commutable with \hat{H} , and idempotent.

As in SFCIS, we have some freedom in choosing our reference for SFPCIS. As will be discussed later, use of ROHF guarantees size-intensivity of computed excitation energies, but static correlation may not be fully taken into account. On the other hand, one can break the spin symmetry in UHF and restore it through SFPCIS procedure to add the missing static correlation. We will examine both possibilities in our benchmark calculations.

The strengths and weaknesses for the methods considered in this work are summarized in Table I.

C. Implementation

We may now derive analytical expressions of Eqs. (6) and (7) for efficient diagonalization of Eq. (5). We should note that, as is the case with SFCIS and CIS, SFPCIS is formally very similar to PCIS in practice except that we do not flip spins in the latter. Therefore, the basic derivation of working equations closely follows that of PCIS.

Let us start with the ground state expectation values,

$$O_0 = \langle \Phi | \hat{O} \hat{P}^s | \Phi \rangle, \quad (8)$$

where $\hat{O} = \hat{H}, \hat{1}$. Here, it should be stressed that the projection \hat{P}^s is meaningful only when operated to determinants with $S_z = m$ with $m \leq s$ (we only consider ROHF and UHF determinants); indeed, for determinants with a multiplicity of $m+1$,

$$\hat{P}^s | \Phi \rangle \equiv 0, \quad (9)$$

because the integration over γ will cancel out (see Eq. (2)). O_0 , therefore, vanishes to zero.

At a first glance, the presence of spin projector thus might seem to complicate the analytical derivation of couplings, Eqs. (6) and (7). One could honestly formulate SFPCIS as (non-SF) restricted active space CI^{48,49} as was indeed done in the original work of SC-SFCIS, i.e., first perform a *pre*-SF excitation from α HOMO to β LUMO, followed by S_z -preserved excitations to produce all the determinants that emerge in SFPCIS. This allows one to explicitly derive the couplings by recognizing closed-shell (a) (Figure 1) as a reference instead of $|\Phi\rangle$, but it would involve matrix elements between doubly substituted projected determinants. It then becomes necessary to construct several different Fock-like matrices for each SFPCIS solution, which is not favorable from a computational view point.

Fortunately, it is possible to directly extract spin-flipped couplings from O_0 . To this end, we consider an infinitesimal rotation on determinant $|\Phi\rangle$ but only in the $\alpha\beta$ spin section,

$$|\Phi + \delta\Phi\rangle = \exp\left[\sum_{i\bar{a}} \Delta_{i\bar{a}} a_{\bar{a}}^\dagger a_i\right] |\Phi\rangle, \quad (10)$$

where Δ is a skew matrix. Note that Eq. (10) is not meaningful as an orbital rotation; it generates a mixture of different S_z states, $m+1, m, m-1, \dots$. Rather, it is a useful mathematical tool for obtaining the coupling terms. Since the variations with respect to $\Delta_{i\bar{a}}$ and the deformed density matrix $\rho_{\bar{a}i} = \langle\Phi|a_{\bar{a}}^\dagger a_i|\Phi\rangle$ are formally equivalent to one another, we perturb O_0 with $|\delta\Phi\rangle$ to second order and obtain

$$\langle\Phi_i^{\bar{a}}|\hat{O}\hat{P}^s|\Phi_j^{\bar{b}}\rangle = \frac{\partial^2 O_0}{\partial \rho_{i\bar{a}} \partial \rho_{\bar{b}j}}. \quad (11)$$

Eq. (11) is exact for any reference determinants. The complete expressions for \mathbf{H} and \mathbf{N} are found in Appendix A.

It is worth noting that the rotation operator $\hat{R}(\Omega)$ is independent of s and m values in Eq. (2). Instead, it is weights that characterize the spin state of the final projected wave function. Thus, one can compute different spin states, $s+1, s+2, \dots$, by simply using $d_{mm}^{s+1}, d_{mm}^{s+2}, \dots$, in SFPCIS (in PCIS, too). This corresponds to diagonalizing different spin blocks of the Hamiltonian matrix in terms of low-spin states, similarly to regular CIS.

Finally, we mention some practical points in use of \hat{P}^s . Since $\hat{S}_z|\Phi_i^{\bar{a}}\rangle = m|\Phi_i^{\bar{a}}\rangle$ and $\hat{O} = \hat{H}, \hat{1}$ are a spin-free operator, we can integrate out α and γ to a constant without loss of generality. Thus, we shall use a simplified operator,

$$\hat{P}^s = \frac{2s+1}{2} \int_0^\pi d\beta d_{mm}^{s*}(\beta) e^{-i\beta\hat{S}_y}, \quad (12)$$

in computing Eq. (11) instead of the full spin-projection operator, to drastically ameliorate the computational cost. For numerical convenience, the integration in Eq. (12) is further discretized into N_{grid} points,

$$\hat{P}^s \approx \sum_g^{N_{\text{grid}}} w_g \hat{R}_g. \quad (13)$$

Since the computation on each grid point is completely independent of one another, one can easily parallelize a SFPCIS calculation efficiently.

D. Orbital invariance

Orbital invariance is a desirable property for a method. It is easy to show that SC-SFCIS depends on the choice of open-shell orbitals of the reference ROHF wave function, ϕ_A and ϕ_B (Figure 1). To see this, consider a unitary rotation between these through rotation angle θ ,

$$\begin{pmatrix} \phi'_A & \phi'_B \end{pmatrix} = \begin{pmatrix} \phi_A & \phi_B \end{pmatrix} \begin{pmatrix} \cos\theta & \sin\theta \\ -\sin\theta & \cos\theta \end{pmatrix}. \quad (14)$$

Although such a rotation will not change the overall space created by $|\Psi_0^S\rangle$ type states shown in Figure 2, it will change $|\Psi_1^S\rangle$ and $|\Psi_2^S\rangle$ because (h1), (h2), (h4), and (h5) do not span the complete set within the open-shell space. For example, determinant (h1), which we abbreviatedly represent as $|\phi_i\phi_A\bar{\phi}_B\bar{\phi}_a\rangle$, will gain additional terms $|\phi_i(\phi_A)^2\bar{\phi}_a\rangle$ and $|\phi_i(\phi_B)^2\bar{\phi}_a\rangle$, i.e., (x1) and (x2) in Figure 3. In order for

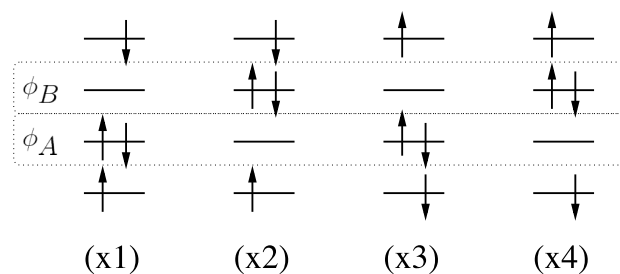


FIG. 3. Additional determinants required to satisfy orbital invariance between ϕ_A and ϕ_B .

a method to be orbital independent, these configurations must either be already redundant or cancel out. Since these determinants are not present in the “unrotated” SC-SFCIS at $\theta = 0^\circ$ and now span a different configuration space when orbitals are rotated, the method is not invariant.

In order to make SC-SFCIS invariant with respect to an open-shell rotation, one thus has to introduce additional variational parameters associated with (x1) and (x2) and their spin-complements (x3) and (x4). This procedure happens to exactly correspond to the SF extended CIS (SF-XCIS) method proposed by Casanova and Head-Gordon,¹⁵ although the motivation of their work was to add some dynamical correlation to SC-SFCIS.

Another way to guarantee the orbital invariance property is to eliminate these additional determinants ((x1)–(x4)) effectively. It is not difficult to verify this is actually the case with SFPCIS. Thanks to the uniqueness of the action of spin projection, \hat{P}^s yields only one well-defined spin state per broken-symmetry determinant. Hence, although there are two singlet CSFs associated with (h), spin-projection generates only one CSF, which is actually a linear combination of the two with fixed weights,

$$\begin{aligned} \hat{P}^{s=0}(\text{h}) &= -(\text{h1}) + (\text{h2}) + 2(\text{h3}) + 2(\text{h}) + (\text{h4}) - (\text{h5}) \\ &\equiv -\frac{1}{2}|\Psi_1^S\rangle + \frac{3}{2}|\Psi_2^S\rangle. \end{aligned} \quad (15)$$

Again, (h1) will still yield additional determinants via a rotation with Eq. (14), but this time they are exactly cancelled out by those from (h2). Similarly, the orbital rotation perturbs (h4), but there is no net effect together with (h5). Here, we used a ROHF reference to make an explicit comparison against SC-SFCIS, but our argument holds for general broken-spin cases.

Therefore, SFPCIS is orbital invariant, wisely choosing only the necessary CSFs as a superposition of $|\Psi_1^S\rangle$ and $|\Psi_2^S\rangle$, which cancels out the open-shell rotation effect. We should also emphasize that SFPCIS is perhaps a minimal approach, and our *ansatz* is more compact than both SC-SFCIS and SF-XCIS. It uses less variational parameters and thereby is strictly upper bound in energy to any possible SC-SFCIS solutions, as will be demonstrated in Section IV. The difference in their energies is, however, explained by a large number of configurations with small CI coefficients added to the latter: the important degeneracy effects that appear in both ground and excited states are assumed to be already accounted for in SFPCIS. Thus, it is expected that both methods would yield comparable accuracy when the residual dynamical correlation is added through a perturbative treatment.

E. Size-consistency and size-intensivity in SFPCIS

Excitation energies are a size-intensive property and should be independent of the system size. It was shown that SF-CIS and SF-XCIS satisfy this condition, while it is well-known that projected methods including PCIS do not obey the size-intensive law in general.^{28,37,50–52} This failure is directly linked to the lack of size-consistency in the projection approaches. In this section, we will follow the discussion presented in Ref. 9 to argue whether SFPCIS can be size-consistent.

A method is said to be size-consistent if the computed energy of two infinitely separated fragments, **A** and **B**, is equal to the sum of energies of each fragment by separate calculations,

$$E_{AB} = E_A + E_B. \quad (16)$$

Here, we restrict our discussion to the case where **A** and **B** are non-interacting at such limit (i.e., no bond-breaking between fragments). The Hamiltonian operator then becomes the sum of two local Hamiltonian operators for the individual fragments,

$$\hat{H} = \hat{H}_A + \hat{H}_B. \quad (17)$$

In order for a method to be size-consistent in this non-interacting limit, its wave function should be separable into a product of two local wave functions,

$$|\Psi\rangle = |\Psi_A\rangle|\Psi_B\rangle. \quad (18)$$

It is well-known that a Slater determinant is of this form, which we define as $|0_A\rangle|0_B\rangle$, where we assume $|0_A\rangle$ is $m = 1$ and $|0_B\rangle$ is $m = 0$. As discussed earlier,³⁸ the spin-projection operator cannot be decomposed locally, and thus \hat{P}^s acts to both **A** and **B** simultaneously. Therefore, the PHF wave function $\hat{P}^s|0_A\rangle|0_B\rangle$ cannot be written as Eq. (18) unless either $|0_A\rangle$ or $|0_B\rangle$ is already spin-adapted,⁵³ in which case the projection operator is only relevant to the broken-symmetry fragment and can be decomposed. PHF, especially the VAP approach, is hence not size-consistent,^{38,52} and neither is PCIS.²⁸

For SFPCIS, however, use of the converged ROHF reference avoids this problem. In this case, $|0_A\rangle$ and $|0_B\rangle$ are high-spin ROHF and closed-shell RHF, respectively. By SF excitations, each fragment can excite one electron within itself, or transfer one electron to the other fragment, and we represent such states as $|\Phi_A\rangle$ and $|\Phi_B\rangle$. In SFPCIS/ROHF, the projected determinant space is thus composed of $\hat{P}^s|\Phi_A\rangle|0_B\rangle$, $\hat{P}^s|0_A\rangle|\Phi_B\rangle$, and $\hat{P}^s|\Phi_A\rangle|\Phi_B\rangle$. Among them, the first space is “local” SFPCIS for **A** because \hat{P}^s does not change closed-shell $|0_B\rangle$. It becomes immediately clear that $\hat{P}^s|\Phi_A\rangle|\Phi_B\rangle$ does not mix with this space due to different electron numbers in **A**. On the other hand, $\hat{P}^s|0_A\rangle|\Phi_B\rangle$ contains determinants with the same number of α and β electrons as does $\hat{P}^s|\Phi_A\rangle|0_B\rangle$, because spin-projection interchanges electron spins between $|\Phi_A\rangle$ and $|0_B\rangle$ (see, for example, Eq. (15)). Given that $|0_B\rangle$ is closed-shell and \hat{H} is separable as in Eq. (17), $\hat{P}^s|0_A\rangle|\Phi_B\rangle$ contains only singly excited determinants in **B**, even after spin-projection. Therefore, this space is orthogonal through \hat{H}_A because the overlap within **B** is zero, and also through \hat{H}_B due to the Brillouin theorem. Overall, $\hat{P}^s|\Phi_A\rangle|0_B\rangle$ is orthogonal to other two spaces through the Hamiltonian operator, so that the Hamiltonian matrix is block-diagonal. Therefore, SFPCIS/ROHF is size-consistent.

Of course, this is only a special case and SFPCIS is in general not size-consistent due to use of the spin-projection operator. Thus, their excitation energies are not rigorously size-intensive. However, it will be shown that this inconsistency in SFPCIS is not as severe as in PCIS, because the correlation effect is in part size-consistent owing to SF excitations.

III. COMPUTATIONAL DETAILS

We have implemented SFPCIS in our in-house quantum chemistry program package. Diagonalization of Eq. (5) is efficiently carried out with the Davidson algorithm for a generalized eigenvalue problem.⁵⁴ We employ $N_{\text{grid}} = 9$ both for SFPCIS and PCIS, which was found sufficient for our test cases. SC-SFCIS and SF-XCIS were also implemented based on SFPCIS by adding additional broken-symmetry determinants to span the appropriate variational space when spin-projected, namely, (h5) for SC-SFCIS, and both (x1) and (x2) in addition for SF-XCIS. The triplet calculations with SF-XCIS further require (h2) because there are three linearly independent triplets. All the calculations for SFCIS, SC-SFCIS, and SF-XCIS in this work start from a high-spin triplet ROHF reference, while for SFPCIS we use both a ROHF determinant and a deformed UHF state of PHF. Reference determinants for SF approaches are selected simply by minimizing its energy, unless otherwise noted. For open-shell orbitals used in SC-SFCIS, we performed diagonalization of the effective Fock matrix parametrized by Guest and Saunders at the end of each ROHF calculation,⁵⁵ which appears to be the one used in the original work. Although we found very small discrepancies between their SC-SFCIS energies and ours in some cases (typically order of 10 μE_h), we concluded that they are attributed to the different numerical conditions employed in each calculation. For full CI (FCI) calculations, we have used GAMESS suite of programs.⁵⁶ We will also present the results of PCIS/PHF.

Finally, we noticed that the rank of the overlap matrix **N**, Eq. (7), is always $M - 1$ in SFPCIS calculations, with M being the size of the matrix. This fact is most naïvely understood as the linear dependence between (c) and (d) in Figure 1 after spin-projection. Nevertheless, such linear dependence poses no issue in actual computations, as it can be easily removed in the Davidson algorithm.

IV. RESULTS AND DISCUSSIONS

A. Orbital dependence: HF

First, we examine orbital dependence in each method. Figure 4 shows the energy of the HF molecule at 1 Å computed with a 6-31G basis.⁵⁷ Here, we take $^3\Sigma$ as the reference and change θ according to Eq. (14). The SC-SFCIS energy at $\theta = 0^\circ$, $-100.009\,119\,E_h$, is almost identical to the value reported by Sears *et al.* ($-100.009\,077\,E_h$).¹¹ It can be seen that the energy dependence is rather severe for the $^1\Sigma$ ground state, giving an energy range ΔE of more than 20 mE_h . On the other hand, the energy of the first singlet excited state $^1\Pi$ is less affected by θ ($\Delta E < 4\,mE_h$), which can cause imbalance in the accuracy of excitation energies. One could optimize

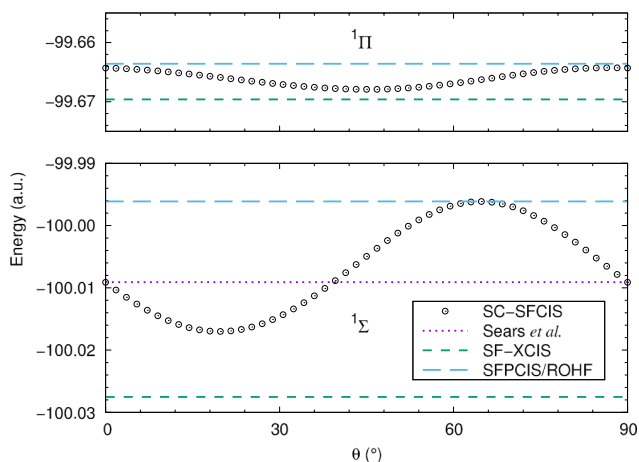


FIG. 4. Energy dependence on orbital rotation θ for HF $^1\Sigma$ (bottom) and $^1\Pi$ (top), computed with a 6-31G basis.

ROHF orbitals so that the ground state is stationary, but this would not guarantee that excited states are also at a minimum, leaving some ambiguity. Hereafter, we will report the SC-SFCIS values at $\theta = 0^\circ$.

From Figure 4, it is also confirmed that both SFCIS/ROHF and SF-XCIS are independent of θ . The former is very close to the maximum energy of SC-SFCIS for each state, but they do not have to coincide in general, e.g., $-99.996\,119$ and $-99.996\,136$, respectively, for $^1\Sigma$. In contrast, SF-XCIS is necessarily lower in energy than the minimum of SC-SFCIS.

B. Ground state: HF

Guided by the earlier work,^{8,11,15} we compare the ground state energies of HF across the nuclear distance. We also use a small 6-31G basis as in Section IV A, because the exact FCI calculation is available and also because static correlation is much less sensitive to the basis set size than is dynamical correlation.

Plotted in Figure 5 are the computed total energies except for SFPCIS/PHF, which is found to be very similar to SFPCIS/ROHF in this particular case. We have also listed the total energies in Appendix B. As expected, the SFPCIS/ROHF energy is always upper bound to SC-SFCIS, but it still adds some correlation effect to SFCIS by bringing it back to the spin-complete regime. However, the correlation energy is

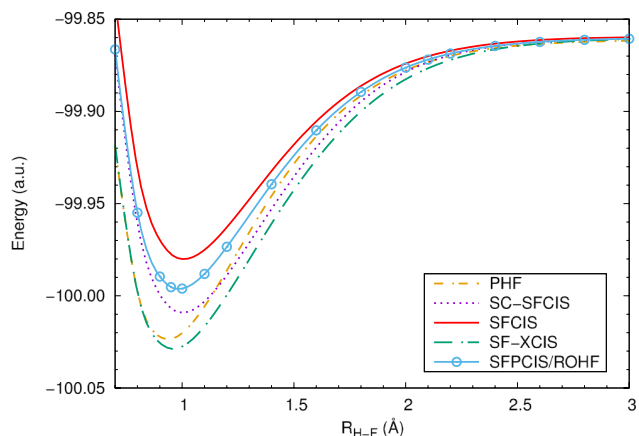


FIG. 5. Potential energy curves of HF with a 6-31G basis.

largely underestimated compared to regular PHF. Since the SFPCIS wave function includes PHF *ansatz*, it has a chance to outperform PHF if the reference occupied orbitals are appropriately chosen. One is thus tempted to optimize the SFPCIS wave function by rotating occupied and virtual orbitals; however, such a biased operation would spoil the essence of the SF approach, because the ground state would be intentionally more preferred than the excited states, and they would be no longer treated on the same footing.

Choosing ROHF or PHF as a reference in SFPCIS does not critically change the results for this system. Although we notice that using SFPCIS/PHF typically lowers the total energy compared to SFPCIS/ROHF, their difference is about 1 mE_h , for example, their energies at 1 Å are $-99.997\,442\text{ E}_h$ and $-99.996\,119\text{ E}_h$, respectively. This is because static correlation is not significant in single bond breaking, and SF excitations can take care of it thoroughly. As we will see later, this is not always true for more strongly correlated systems.

Figure 6 shows the energy errors from FCI in kcal/mol. Previously, it has been reported that a second-order perturbation correction to SFCIS (SF-CIS(D)) is a very good approximation to FCI for this system.^{9,10} We have also recently shown that PHF gives excellent results when a similar correction is added (labeled as EMP2).⁵⁸ Therefore, one can expect that SFPCIS can be also extended in a similar way to include dynamical correlation effects, and it is plausible that its performance is better than SF-CIS(D) because the zeroth order wave function (SFPCIS) is more appropriate than broken-symmetry SFCIS.

C. Conical intersection: H₃

Here, we would like to give an example where a balanced treatment of both ground and excited states is crucial: conical intersection. We take the simplest trihydrogen molecule for our test case, as a proof of principle.⁵⁹ Note that this system contains an odd number of electrons, so SC-SFCIS and SF-XCIS are not applicable in their current formulations. For SFPCIS, we consider SF excitations that involve quartet to doublet with a reference of $|s; m\rangle = |\frac{3}{2}; \frac{3}{2}\rangle$. When the structure becomes an equilateral triangle, the lowest two doublet states, $|D_0\rangle$ and $|D_1\rangle$, are degenerate. We thus first search the optimal

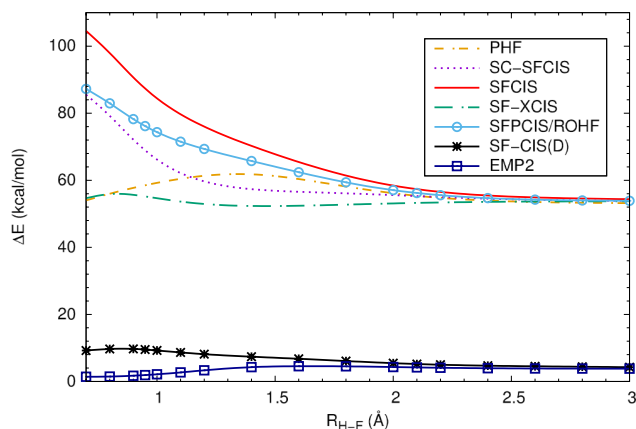


FIG. 6. Error from FCI in kcal/mol for the HF molecule computed with a 6-31G basis.

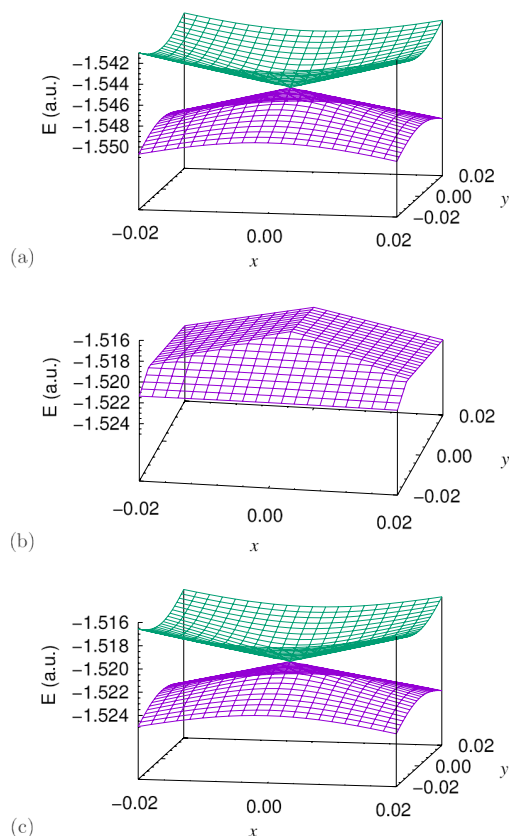


FIG. 7. Conical intersection of H_3 : (a) FCI, (b) PCIS, (c) SFPCIS. The basis set used is 6-31G**.

bond length R_{H-H} for such D_{3h} structure that yields the lowest energy. With a 6-31G** basis, it is determined that $R_{H-H} = 1.075, 1.212$, and 1.210 Å for FCI, PCIS (i.e., PHF), and SFPCIS, respectively. We then displace one H atom parallelly (x) and vertically (y) to other two hydrogen atoms and compute the potential energy surfaces of the lowest two states as shown in Figure 7. FCI clearly shows a conical intersection as expected. The PCIS results are disappointing; the $|D_1\rangle$ state was not obtained and thus there is no conical intersection. This failure is simply attributed to the absence of explicit double substitutions in PCIS. SFPCIS includes such substitutions effectively through SF and reproduces the correct shape of energy surfaces.

We should emphasize that the success of SFPCIS in capturing a conical intersection essentially owes to SF, rather than spin-projection. For this simple case, the energy surfaces of SFCIS are also similar to FCI (not shown) as spin-contamination is found to be small enough for both $|D_0\rangle$ and $|D_1\rangle$ ($\langle\hat{S}^2\rangle \sim 0.755$). The correlation energy acquired by spin-projection in SFPCIS is about ~ 3 mE_h, while the “residual” dynamical correlation (i.e., the energy difference between FCI and SFPCIS) remains to be 26 mE_h. However, importantly, these results show that spin-projection does not undermine the balanced treatment of SF, while clearly being a better alternative to the PCIS model.

D. Excited state: N_2

N_2 is also a challenging case because it requires up to sextuple excitations in order to break its triple bond. Hence,

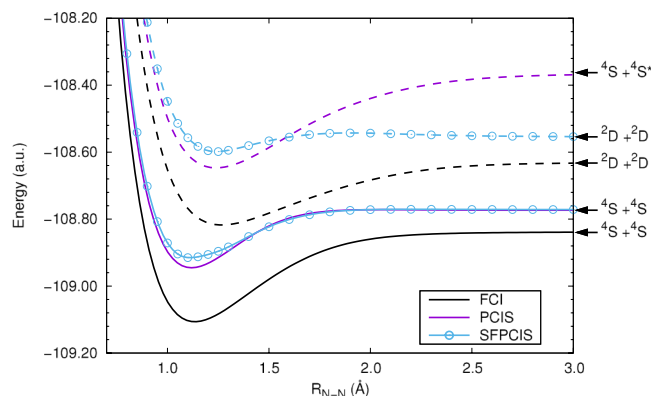


FIG. 8. N_2 potential energy curves computed with a 6-31G basis. The solid curves are $1\Sigma_g^+$ and the dashed curves are $1\Pi_g$.

none of the conventional SF methods with singles and doubles can handle the ground state of this system. Its excited states are even more complicated especially when the bond is stretched, where the spectrum becomes highly dense. Of course, all of these excitations cannot be treated unless one adopts a complete active space.

We use a PHF $|1; 1\rangle$ state as a SFPCIS reference, with $2\sigma_g$ and $2\sigma_u$ orbitals chosen as the high-spin open-shell orbitals for SF, while π_x and π_y bonds are treated by spin-symmetry breaking and restoration (the principle axis is z). The basis set employed is 6-31G, and the 1s orbitals are not correlated in FCI calculations.

Figure 8 illustrates the potential energy curves of the ground state $1\Sigma_g^+$ and the excited state $1\Pi_g$, which is the two lowest degenerate excited states in both PCIS and SFPCIS across the almost entire nuclear coordinate. The ground state is correctly captured both with PCIS (PHF) and SFPCIS. The latter slightly underestimates dynamical correlation compared to the former at equilibrium, but both successfully dissociate to the $N(^4S) + N(^4S)$ limit.⁶⁰ On the other hand, all the other low-lying singlet states including $1\Pi_g$ must disassociate to $N(^2D) + N(^2D)$, as is the case with FCI and SFPCIS. PCIS approximates the excitation energy very well in the vicinity of equilibrium, but it incorrectly gives $N(^4S) + N(^4S^*)$ at separation, where $4S^* = |1s^2 2s 2p_x^2 2p_y 2p_z\rangle$. To show some numerics, we tabulate excitation energies at equilibrium (1.098 Å) and dissociation in Table II. Although not shown in Figure 8, both SFCIS and SF-XCIS excitation energies become unphysically small as the molecule dissociates, because of the closing gap.

We should note other possibilities in the choice of open-shell orbitals in SFPCIS. For example, one could utilize $\pi_{x,u}$ and $\pi_{x,g}$ as the SF pair. We found that the energy diagram of $1\Sigma_g^+$ did not change drastically with this choice. However, it violated the symmetry between π_x and π_y bonds and thus two $1\Pi_g$ states were split, although they both dissociated to the correct $N(^2D) + N(^2D)$ limit. This indicates that, in general,

TABLE II. Excitation energies of N_2 (eV). The basis set used is 6-31G.

R_{N-N} (Å)	SFCIS	PCIS	SFPCIS	FCI
1.098	8.23	8.44	8.97	8.42
3.0	1.08	11.01	5.93	5.61

one has to be careful about what state is used as a reference, which unfortunately makes the method not completely black-box, one of the well-known drawbacks of SF approaches.

E. Static correlation: H_4

In this section, we examine our method for distorted square H_4 as a rich source of strong static correlation—beyond single orbital entanglement. This small system consists of two identical H_2 molecules symmetrically placed on a circle with a radius of $R = 1.738 \text{ \AA}$, where the bond length of each molecule is characterized by a central angle θ .⁶¹ At $\theta = 90^\circ$, pairs of H_2 interchange, and their electronic structures become fully entangled. As a result, standard single reference methods exhibit a pronounced derivative discontinuity in the ground state potential energy curve, indicating two sets of H_2 pairs are not treated equally.^{61,62}

Not only does the ground state pose a theoretical challenge but also of particular interest are their correlated excited states and the interplay between (nearly)degenerate states. We will, therefore, apply SF models to this system in order to investigate their applicability and limitations. In what follows, we will use the Dunning DZP basis,^{63,64} and note $|S_n\rangle$ and $|T_n\rangle$ to mean n th excited singlet and triplet states of exact FCI (thus $|S_0\rangle$ is the ground state).

1. Singlet

Figure 9 shows the potential energy curves of the low-lying singlet states of SFCIS, SF-XCIS, PCIS, and SFPCIS. On the top panel, the correlation energy in the $|S_0\rangle$ states of SFCIS and SF-XCIS (either the first or second state depending on θ) is significantly underestimated, and the two curves are virtually indistinguishable from one another; additional single excitations in SF-XCIS bring no correlation. This strongly implies that the residual correlation missed in both methods is purely static, which is also evident from the derivative discontinuities. SFCIS cannot predict the $|S_1\rangle$ state, while qualitatively reproducing $|S_2\rangle$. However, this solution is found to be significantly spin-contaminated, $\langle S^2 \rangle \sim 1$ across the entire coordinate and therefore the physical meaning of this state is questionable. On the other hand, SF-XCIS does capture $|S_1\rangle$ quite well but incorrectly predicts it as the ground state around $65^\circ < \theta < 115^\circ$, indicating that its correlation effects in the first and second states are badly imbalanced. For $|S_2\rangle$, SF-XCIS outperforms SFCIS by including additional electron correlations.

The bottom panel of Figure 9 presents the PCIS and SFPCIS results for singlet states. PCIS approximates the strongly correlated $|S_0\rangle$ state very well via spin-projection. However, it does not account for the lowest excited state $|S_1\rangle$, because it requires doubly excited configurations in the projected CI model, similar to the case we have seen in H_3 . We find that SFPCIS does an excellent job for all the states if we use a PHF triplet reference $|1; 1\rangle$. It reproduces both $|S_0\rangle$ and $|S_1\rangle$ states even quantitatively, accurately predicting the gap between $|S_0\rangle$ and $|S_1\rangle$ at $\theta = 90^\circ$ to be 8.29 kcal/mol, whereas the FCI value is 8.38 kcal/mol. The description of $|S_2\rangle$, however, remains only qualitative as in all other methods, and extra correlations are needed.

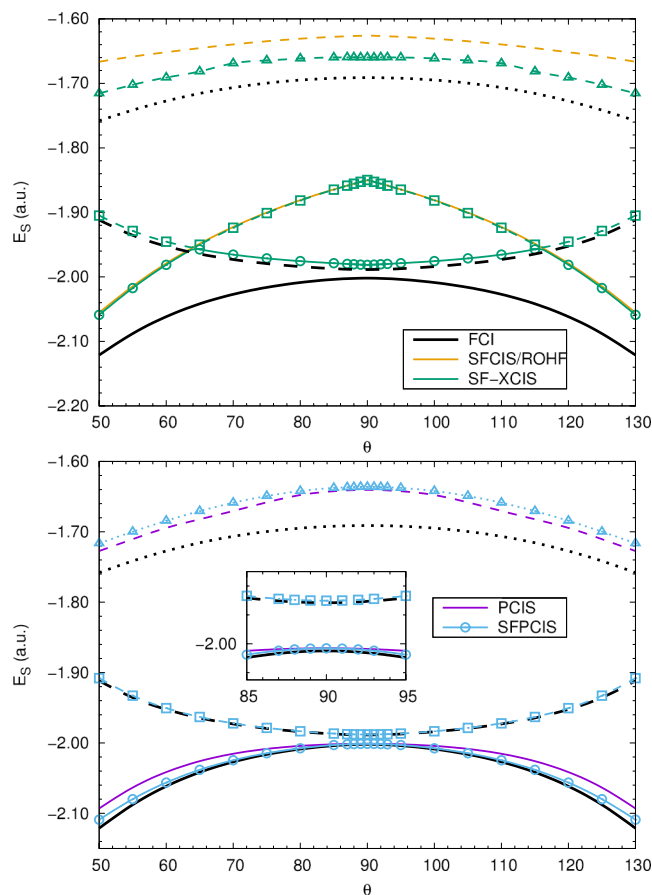


FIG. 9. Potential energy curves of low-lying singlet states in H_4 as a function of coordinate θ . The basis set used is DZP. Solid, dashed, and dotted lines correspond to the first, second, and third lowest solutions of each method.

2. Triplet

As discussed in Section II C, different spin descriptions in SFPCIS can be achieved by changing the “weights” in the projection operator. To demonstrate the validity of this technique, we further investigate triplet states of H_4 , which we found also display complicated electronic structures.

In Figure 10, we plot three lowest triplet states of FCI, SF-XCIS, and SFPCIS. We now omit SFCIS and PCIS from our discussion as their excitation energies are found at a much higher energy region. The energies of the reference triplet states $|1; 1\rangle$, i.e., ROHF and PHF for SF-XCIS and SFPCIS, respectively, are also shown.

It is noticeable that one of the three SF-XCIS triplets simply goes back to the reference ROHF state as a low-spin triplet. This feature is usually desirable, because in the exact theory, high-spin and low-spin triplets are energetically degenerate in the absence of magnetic fields. However, in the present case, the description of the ROHF reference is unfortunately incorrect; the kink at $\theta = 90^\circ$ is due to the failure of the single reference ROHF, implying $|T_1\rangle$ is also highly multireference in nature. FCI predicts a conical intersection-like behavior between two *excited* states, $|T_2\rangle$ and $|T_3\rangle$. SF-XCIS, on the other hand, instead gives an avoided crossing with a small gap of 2.86 kcal/mol.

SFPCIS shows better agreement with FCI for triplet cases as well (lower panel). It is found that the potential energy

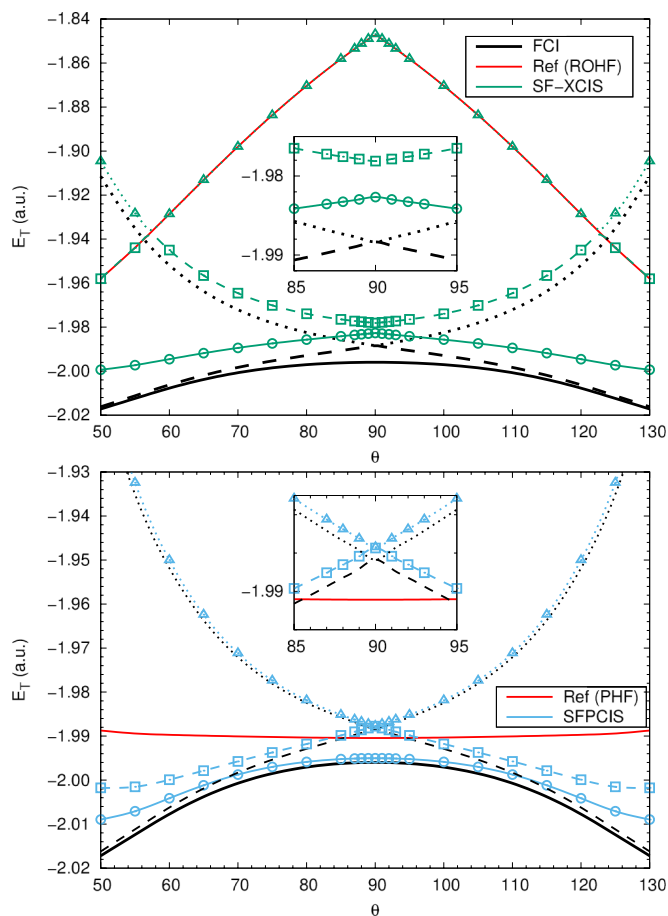


FIG. 10. Same as Figure 9 but for triplet states.

curve of the PHF reference $|1; 1\rangle$ largely underestimates the correlation energy of $|T_1\rangle$, and yet SFPCIS gives qualitative descriptions of all the three states with some dynamical correlation captured by SF excitations. Again, SFPCIS may not be accurate enough for quantitative arguments; the tails of $|T_1\rangle$ and $|T_2\rangle$ are too shallow. It is, nevertheless, remarkable that the complete degeneracy between $|T_2\rangle$ and $|T_3\rangle$ is well reproduced at $\theta = 90^\circ$. Overall, these results show the appropriate “static” character of strongly correlated excited states earned through spin-flip and spin-projection.

F. Numerical assessment for size-intensivity

So far, we have seen some encouraging features of SFPCIS, outperforming original SFCIS and PCIS in many ways. However, the method is surely not without drawbacks. In fact, we discussed in Section II E that SFPCIS is not, in general, size-intensive if one employs a broken-symmetry reference, because of the “size-inconsistent” action of a projection operator. To see how this affects the results, we use two H_2 molecules at infinite separation with a bond length of 1 Å to compare with the monomer. The basis set used is 6-31G.

In Table III, we list the excitation energies of $B^1\Sigma_u^+ \leftarrow X^1\Sigma_g^+$ both for the monomer H_2 and the dimer $(H_2)_2$. Since the PCIS results depend on the system size,²⁸ the excitation energy of $(H_2)_2$ is found to be lower than that of H_2 by 0.312 eV. When PHF is used as a reference, SFPCIS also exhibits a discrepancy

TABLE III. Excitation energies in eV of H_2 and its infinitely separated dimer for size-intensive test with a 6-31G basis.

	SFCIS	PCIS	SFPCIS ^a	SFPCIS ^b	FCI
H_2	13.582	13.469	13.349	13.349	13.288
$(H_2)_2$	13.582	13.157	13.361	13.349	13.288
Error	0.000	0.312	-0.012	0.000	0.000

^aThe PHF reference is used. For H_2 , it is identical to the result with the ROHF reference.

^bThe ROHF reference is used.

in the computed energies. However, this undesired effect is somewhat ameliorated and compensated by SF, which itself is a size-consistent operation if the CI wave function is limited to include no more than single non-SF excitations and the Brillouin condition is satisfied.²⁹ As a result, the energy error of SFPCIS/PHF is only -0.012 eV, which is greatly reduced compared to PCIS. SFPCIS can be further made size-intensive by using a ROHF reference (Table III), although this would then limit the ability of SFPCIS in capturing more general static correlation.

Previously, it was reported that singly excited states in the PCIS model can eventually approach to those in regular CIS at the thermodynamic limit, while doubly excited states remain unique.²⁸ On the other hand, as is evident from Table III, the SFPCIS excitation energies will not coincide those of SFCIS at such limit. This fact is understood as follows. The SFCIS ground state is usually much less spin-contaminated compared to excited states, which are almost always found to be an equal mixture of singlet and triplet states. Hence, the spin-projection effect is far more important in excited states. This result is intriguing because even for a very large system, spin-contamination can play an important role for the quality of the obtained results, and therefore spin-projection would make a clear distinction between SFCIS and SFPCIS.

V. CONCLUDING REMARKS

The spin-flip and spin-projection approaches both tackle the long-standing difficulty in treating static correlation in a cost-effective manner. It is known that they have different strengths and weaknesses: while SFCIS is spin-incomplete and its excitation energies can be unreliable, PCIS is not capable of describing near-degeneracy between the ground and excited states, typically found as a conical intersection in real systems. In this paper, we described a hybrid of the two schemes, termed SFPCIS, in order to remedy, or at least to mitigate, the deficiencies in each method as a minimal approach. It was shown that our method is orbital invariant, is applicable to any spin states, and removes higher spin-contamination to gain general static correlation, at a similar computational scaling to SFCIS and PCIS.

Although both SC-SFCIS and SF-XCIS are no doubt a better alternative to the spin-contaminated SFCIS, they still lack major dynamical correlation. Nonetheless, there has been almost no progress on the development of a perturbative approach based on them. This is perhaps because the resultant wave functions are far too complicated, hindering a straightforward generalization of the SF-CIS(D) approach. We deem that, once the spin-coupled determinants are

manually introduced, the simplicity of single reference picture in SFCIS is no longer available, necessitating to adopt the expensive multireference perturbation theory. In this regard, SFPCIS can be still considered a single reference theory, whose multireference character is partly obtained through the spin-projection operator. Therefore, it is quite hopeful that introducing a perturbative correction to SFPCIS would not add significant complexity to the model.⁵⁸ Furthermore, the proposed scheme can be easily extended to include explicit double substitutions,⁹ although the implementation is slightly more complicated. We are currently working along these directions.

Finally, we should note that one has to carefully choose the appropriate open-shell orbitals in all the SF approaches, and SFPCIS is no exception. Typically, such an orbital choice is made based on chemical intuition of the target system (e.g., bonding and anti-bonding orbitals) as seen in Section IV D. Thus, a great care has to be taken for a system whose chemical property is unknown *a priori*. Nonetheless, it is hoped that with an appropriate reference SFPCIS can offer the correct description of both ground and excited states for strongly correlated systems, especially when dynamical correlation is incorporated.

ACKNOWLEDGMENTS

The author is indebted to Seiichiro Ten-no sensei for helpful discussions and to Motoyuki Uejima for a critical reading of this paper. This work was supported in FLAG-SHIP2020 by MEXT as the priority issue 5 (Development of new fundamental technologies for high-efficiency energy creation, conversion/storage and use) to be tackled by using the Post K Computer. We partially used computational resources of the K computer provided by RIKEN Advanced Institute for Computational Science through the HPCI System Research project (No. hp150278).

APPENDIX A: MATRIX ELEMENTS

Here, we present the matrix elements for SFPCIS based on Eq. (11). The expressions are very similar to those of PCIS described in Ref. 28.

First, we briefly review PHF to define our notations in the molecular orbital basis of $|\Phi\rangle$. Using Eq. (8), the PHF energy is given by

$$E_0 = \frac{H_0}{N_0}. \quad (\text{A1})$$

Each projected coupling can be discretized based on Eq. (13),

$$\begin{aligned} H_0 &= \langle \Phi | \hat{H} \hat{P}^s | \Phi \rangle \\ &= \sum_g w_g n_g E_g, \end{aligned} \quad (\text{A2})$$

$$\begin{aligned} N_0 &= \langle \Phi | \hat{P}^s | \Phi \rangle \\ &= \sum_g w_g n_g, \end{aligned} \quad (\text{A3})$$

where the rotated overlap coupling $n_g = \langle \Phi | \hat{R}_g | \Phi \rangle$ can be written in terms of the rotation matrix, \mathbf{R}_g , as

$$n_g = \det \mathbf{R}_g^{oo}, \quad (\text{A4})$$

with oo being the occupied-occupied block. We will use a similar notation for virtual space v . Using generalized Wick's theorem,³⁶ the Hamiltonian coupling $E_g = \langle \Phi | \hat{H} \hat{R}_g | \Phi \rangle / \langle \Phi | \hat{R}_g | \Phi \rangle$ is given by

$$E_g = \sum_{pq} h_{pq}(\rho_g)_{qp} + \frac{1}{2} \sum_{pqrs} \langle pr || qs \rangle (\rho_g)_{qp} (\rho_g)_{sr}, \quad (\text{A5})$$

where h_{pq} and $\langle pr || qs \rangle$ are standard notations for one-electron and two-electron integrals, and the transition density matrix

$$(\rho_g)_{qp} = \frac{\langle \Phi | a_p^\dagger a_q \hat{R}_g | \Phi \rangle}{\langle \Phi | \hat{R}_g | \Phi \rangle} \quad (\text{A6})$$

is defined in the MO basis as

$$\rho_g = \begin{pmatrix} \mathbf{1}^{oo} & \mathbf{0}^{ov} \\ \mathbf{R}_g^{vo} (\mathbf{R}_g^{oo})^{-1} & \mathbf{0}^{vv} \end{pmatrix}. \quad (\text{A7})$$

As mentioned in Section II C, the Hamiltonian and overlap elements of SFPCIS can be obtained as derivatives as Eq. (11). If we further define

$$\mathbf{W}_g = \begin{pmatrix} (\mathbf{R}_g^{oo})^{-1} & (\mathbf{R}_g^{oo})^{-1} \mathbf{R}_g^{ov} \\ \mathbf{R}_g^{vo} (\mathbf{R}_g^{oo})^{-1} & (\mathbf{R}_g^{vv, \dagger})^{-1} \end{pmatrix}, \quad (\text{A8})$$

$$(\mathbf{F}_g)_{pq} = h_{pq} + \sum_{pqrs} \langle pr || qs \rangle (\rho_g)_{sr}, \quad (\text{A9})$$

the SFPCIS matrix elements are conveniently written as

$$\begin{aligned} H_{j\bar{b}}^{i\bar{a}} &= \sum_g w_g n_g \left[E_g \{ (\mathbf{W}_g)_{\bar{a}\bar{b}} (\mathbf{W}_g)_{ji} + (\mathbf{W}_g)_{\bar{a}i} (\mathbf{W}_g)_{j\bar{b}} \} \right. \\ &\quad + (\tilde{\mathcal{F}}_g)_{\bar{a}i} (\mathbf{W}_g)_{j\bar{b}} + (\tilde{\mathcal{F}}_g)_{j\bar{b}} (\mathbf{W}_g)_{\bar{a}i} \\ &\quad + (\tilde{\mathcal{F}}_g)_{\bar{a}\bar{b}} (\mathbf{W}_g)_{ji} - (\tilde{\mathcal{F}}_g)_{ji} (\mathbf{W}_g)_{\bar{a}\bar{b}} \\ &\quad \left. + \sum_{pqrs} (\mathbf{U}_g)_{\bar{a}p} (\mathbf{V}_g)_{qi} (\mathbf{U}_g)_{jr} (\mathbf{V}_g)_{s\bar{b}} \langle pr || qs \rangle \right], \end{aligned} \quad (\text{A10})$$

$$N_{j\bar{b}}^{i\bar{a}} = \sum_g w_g n_g [(\mathbf{W}_g)_{\bar{a}\bar{b}} (\mathbf{W}_g)_{ji} + (\mathbf{W}_g)_{\bar{a}i} (\mathbf{W}_g)_{j\bar{b}}], \quad (\text{A11})$$

where we have introduced

$$\tilde{\mathcal{F}}_g = \mathbf{U}_g \mathbf{F}_g \mathbf{V}_g \quad (\text{A12})$$

with left- and right-transformation matrices

$$\mathbf{U}_g = \begin{pmatrix} (\mathbf{R}_g^{oo})^{-1} & \mathbf{0}^{ov} \\ -\mathbf{R}_g^{vo} (\mathbf{R}_g^{oo})^{-1} & \mathbf{1}^{vv} \end{pmatrix}, \quad (\text{A13})$$

$$\mathbf{V}_g = \begin{pmatrix} \mathbf{1}^{oo} & \mathbf{0}^{ov} \\ \mathbf{R}_g^{vo} (\mathbf{R}_g^{oo})^{-1} & (\mathbf{R}_g^{vv, \dagger})^{-1} \end{pmatrix}. \quad (\text{A14})$$

Note that our definition of $\tilde{\mathcal{F}}_g$ in Eq. (A12) is different from the one given in the previous work in that it has effective oo and vv blocks.

APPENDIX B: TOTAL ENERGIES OF THE HF MOLECULE

Table IV shows the total energies of the HF molecule with a 6-31G basis (see Section IV B).

TABLE IV. Total energies of the HF molecule with a 6-31G basis set (E_h).

R_{HF} (Å)	PHF	SFCIS ^a	SC-SFCIS ^b	SF-XCIS	SFPCIS/ROHF	SFPCIS/PHF	FCI
0.7	-99.919 426	-99.838 867	-99.869 187	-99.918 381	-99.866 443	-99.867 355	-100.005 489
0.8	-99.997 910	-99.931 028	-99.960 866	-99.998 056	-99.954 932	-99.956 079	-100.087 139
0.9	-100.022 253	-99.969 754	-99.999 311	-100.025 560	-99.989 550	-99.990 849	-100.114 251
0.95	-100.023 462	-99.977 465	-100.006 841	-100.028 744	-99.995 319	-99.996 643	-100.116 698
1.0	-100.020 247	-99.980 048	-100.009 119	-100.027 523	-99.996 119	-99.997 442	-100.114 621
1.1	-100.005 791	-99.975 117	-100.003 046	-100.016 616	-99.988 151	-99.989 434	-100.102 115
1.2	-99.986 188	-99.962 797	-99.988 842	-99.999 577	-99.973 437	-99.974 662	-100.083 938
1.2764	-99.970 316	-99.951 334	-99.975 513	-99.984 890	-99.960 492	-99.961 667	-100.068 708
1.4	-99.945 835	-99.932 297	-99.952 882	-99.960 873	-99.939 508	-99.940 596	-100.044 285
1.6	-99.913 542	-99.905 437	-99.919 599	-99.926 227	-99.910 307	-99.911 252	-100.009 752
1.8	-99.891 413	-99.886 214	-99.894 653	-99.900 029	-99.889 445	-99.890 267	-99.984 078
2.0	-99.877 735	-99.874 100	-99.878 632	-99.882 582	-99.876 270	-99.877 004	-99.967 201
2.1	-99.873 252	-99.870 094	-99.873 389	-99.876 625	-99.871 911	-99.872 615	-99.961 487
2.2	-99.869 916	-99.867 100	-99.869 540	-99.872 118	-99.868 657	-99.869 337	-99.957 183
2.4	-99.865 674	-99.863 278	-99.864 782	-99.866 301	-99.864 504	-99.865 155	-99.951 656
2.6	-99.863 448	-99.861 278	-99.862 393	-99.863 221	-99.862 319	-99.862 955	-99.948 741
2.8	-99.862 302	-99.860 285	-99.861 206	-99.861 633	-99.861 190	-99.861 819	-99.947 238
3.0	-99.861 711	-99.859 837	-99.860 610	-99.860 821	-99.860 607	-99.861 233	-99.946 465
3.2	-99.861 019	-99.859 656	-99.860 304	-99.860 403	-99.860 303	-99.860 926	-99.946 065
3.4	-99.861 071	-99.859 581	-99.860 143	-99.860 188	-99.860 141	-99.860 767	-99.945 857

^aROHF reference.^b $\theta = 0$ values using the Guest-Saunders open-shell orbitals. Note that our numbers are slightly different from those in Ref. 11.

- ¹C. D. Sherrill, *J. Chem. Phys.* **132**, 110902 (2010).
- ²S. R. White, *Phys. Rev. Lett.* **69**, 2863 (1992).
- ³G. K.-L. Chan and S. Sharma, *Annu. Rev. Phys. Chem.* **62**, 465 (2011).
- ⁴V. Anisimov and Y. Izyumov, *Electronic Structure of Strongly Correlated Materials* (Springer, Berlin, 2010).
- ⁵T. Tsuchimochi and G. E. Scuseria, *J. Chem. Phys.* **131**, 121102 (2009).
- ⁶P. A. Limacher *et al.*, *J. Chem. Theory Comput.* **9**, 1394 (2013).
- ⁷T. Stein, T. M. Henderson, and G. E. Scuseria, *J. Chem. Phys.* **140**, 214113 (2014).
- ⁸A. I. Krylov, *Chem. Phys. Lett.* **338**, 375 (2001).
- ⁹A. I. Krylov, *Chem. Phys. Lett.* **350**, 522 (2001).
- ¹⁰A. I. Krylov and C. D. Sherrill, *J. Chem. Phys.* **116**, 3194 (2002).
- ¹¹J. S. Sears, C. D. Sherrill, and A. I. Krylov, *J. Chem. Phys.* **118**, 9084 (2003).
- ¹²S. V. Levchenko and A. I. Krylov, *J. Chem. Phys.* **120**, 175 (2004).
- ¹³S. V. Levchenko, T. Wang, and A. I. Krylov, *J. Chem. Phys.* **122**, 224106 (2005).
- ¹⁴A. I. Krylov, *Acc. Chem. Res.* **32**, 83 (2006).
- ¹⁵D. Casanova and M. Head-Gordon, *J. Chem. Phys.* **129**, 064104 (2008).
- ¹⁶P. U. Manohar and A. I. Krylov, *J. Chem. Phys.* **129**, 194105 (2008).
- ¹⁷Y. Shao, M. Head-Gordon, and A. I. Krylov, *J. Chem. Phys.* **118**, 4807 (2003).
- ¹⁸F. Wang and T. Ziegler, *J. Chem. Phys.* **122**, 074109 (2005).
- ¹⁹Y. A. Bernard, Y. Shao, and A. I. Krylov, *J. Chem. Phys.* **136**, 204103 (2012).
- ²⁰Z. Li and W. Liu, *J. Chem. Phys.* **136**, 024107 (2012).
- ²¹L. V. Slipchenko and A. I. Krylov, *J. Chem. Phys.* **117**, 4694 (2002).
- ²²L. V. Slipchenko, T. E. Munsch, P. G. Wenthold, and A. I. Krylov, *Angew. Chem., Int. Ed.* **43**, 742 (2004).
- ²³N. Minezawa and M. S. Gordon, *J. Phys. Chem. A* **113**, 12749 (2009).
- ²⁴M. Huix-Rotlant *et al.*, *Phys. Chem. Chem. Phys.* **12**, 12811 (2010).
- ²⁵N. Minezawa and M. S. Gordon, *J. Phys. Chem. A* **115**, 7901 (2011).
- ²⁶D. Maurice and M. Head-Gordon, *Int. J. Quantum Chem.* **56**, 361 (1995).
- ²⁷T. Tsuchimochi and G. E. Scuseria, *J. Chem. Phys.* **133**, 141102 (2010).
- ²⁸T. Tsuchimochi and T. Van Voorhis, *J. Chem. Phys.* **142**, 124103 (2015).
- ²⁹D. Casanova, L. V. Slipchenko, A. I. Krylov, and M. Head-Gordon, *J. Chem. Phys.* **130**, 044103 (2009).
- ³⁰D. Casanova and M. Head-Gordon, *Phys. Chem. Chem. Phys.* **11**, 9779 (2009).
- ³¹D. Casanova, *J. Chem. Phys.* **137**, 084105 (2012).
- ³²D. Casanova, *J. Comput. Chem.* **34**, 720 (2013).
- ³³F. Bell, P. M. Zimmerman, D. Casanova, M. Golldey, and M. Head-Gordon, *Phys. Chem. Chem. Phys.* **15**, 358 (2013).
- ³⁴P.-O. Löwdin, *Phys. Rev.* **97**, 1509 (1955).
- ³⁵R. Lefebvre and R. Prat, *Chem. Phys. Lett.* **1**, 388 (1967).
- ³⁶P. Ring and P. Schuck, *The Nuclear Many-Body Problem* (Springer-Verlag, Berlin, 1980).
- ³⁷G. E. Scuseria, C. A. Jiménez-Hoyoz, T. M. Henderson, K. Samanta, and J. K. Ellis, *J. Chem. Phys.* **135**, 124108 (2011).
- ³⁸C. A. Jiménez-Hoyoz, T. M. Henderson, T. Tsuchimochi, and G. E. Scuseria, *J. Chem. Phys.* **136**, 164109 (2012).
- ³⁹K. W. Schmid, R.-R. Zheng, F. Grümmner, and A. Faessler, *Nucl. Phys. A* **499**, 63 (1989).
- ⁴⁰C. A. Jiménez-Hoyoz, R. Rodríguez-Guzmán, and G. E. Scuseria, *J. Chem. Phys.* **139**, 204102 (2013).
- ⁴¹B. G. Levine, C. Ko, J. Quenneville, and T. J. Martínez, *Mol. Phys.* **104**, 1039 (2006).
- ⁴²A. Szabo and N. S. Ostlund, *Modern Quantum Chemistry: Introduction to Advanced Electronic Structure Theory* (Dover Publications, Mineola, NY, 1996).
- ⁴³I. Mayer, J. Ladik, and G. Biczó, *Int. J. Quantum Chem.* **7**, 583 (1973).
- ⁴⁴I. Mayer, *Adv. Quantum Chem.* **12**, 189 (1980).
- ⁴⁵H. B. Schlegel, *J. Chem. Phys.* **84**, 4530 (1986).
- ⁴⁶P. J. Knowles and N. C. Handy, *J. Chem. Phys.* **88**, 6991 (1988).
- ⁴⁷L. M. Thompson and H. P. Hratchian, *J. Chem. Phys.* **141**, 034108 (2014).
- ⁴⁸P. A. Malmqvist, A. Rendell, and B. O. Roos, *J. Phys. Chem.* **94**, 5477–5482 (1990).
- ⁴⁹J. Olsen, B. O. Roos, P. Jørgensen, and H. J. A. Jensen, *J. Chem. Phys.* **89**, 2185–2192 (1988).
- ⁵⁰I. I. Ukrainsky, *Int. J. Quantum Chem.* **6**, 473 (1972).
- ⁵¹O. Castaño and P. Karadakov, *Chem. Phys. Lett.* **130**, 123 (1986).
- ⁵²T. M. Henderson and G. E. Scuseria, *J. Chem. Phys.* **139**, 234113 (2013).
- ⁵³T. Tsuchimochi and G. E. Scuseria, *J. Chem. Phys.* **134**, 064101 (2011).
- ⁵⁴E. R. Davidson, *J. Comput. Phys.* **17**, 87 (1975).
- ⁵⁵F. Guest and V. R. Saunders, *Mol. Phys.* **28**, 819 (1974).
- ⁵⁶M. W. Schmidt *et al.*, *J. Comput. Chem.* **14**, 1347 (1993).
- ⁵⁷W. J. Hehre, R. Ditchfield, and J. A. Pople, *J. Chem. Phys.* **56**, 2257 (1972).
- ⁵⁸T. Tsuchimochi and T. Van Voorhis, *J. Chem. Phys.* **141**, 164117 (2014).
- ⁵⁹B. Kaduk and T. Van Voorhis, *J. Chem. Phys.* **133**, 061102 (2010).
- ⁶⁰Rigorously speaking, these are not the same limit due to the lack of size-consistency. However, for this case, the energy errors at $R_{N-N} = 1000$ Å with respect to the energy sum of atomic fragments are small enough: $E_{PHF} = -108.773\,289$ and $E_{SFPCIS} = -108.771\,238$, while $2E_{PHF}(N(^4S)) = -108.773\,296$.
- ⁶¹T. Van Voorhis and M. Head-Gordon, *J. Chem. Phys.* **113**, 8873 (2000).
- ⁶²D. Kats and F. R. Manby, *J. Chem. Phys.* **139**, 021102 (2013).
- ⁶³S. Huzinaga, *J. Chem. Phys.* **42**, 1293 (1965).
- ⁶⁴T. H. Dunning, *J. Chem. Phys.* **53**, 2823 (1970).